Implementation and Verification of V2G Control Schemes on Multiple Electric Vehicles

Hidekuni Toda, Yutaka Ota, Tatsuhito Nakajima
Department of Electrical and Electronic Engineering
Tokyo City University
Tokyo, Japan
g1781343@tcu.ac.jp

Ken-ichi Kawabe
Department of Electrical and Electronic Engineering
Tokyo Institute of Technology
Tokyo, Japan

Akihiko Yokoyama
Department of Advanced Energy
The University of Tokyo
Tokyo, Japan

Abstract—**The regulation market is scheduled to be launched in 2020, distributed generations and energy storages could participate to the market. Massive pure plug-in electric vehicles (PEV) would be on the road, the potential of the V2G is also dramatically increasing toward 2020. In this paper, the proposed V2G control schemes is implemented to the actual PEV and the V2G capable charging system as a first V2G system in Japan. Accuracy of the grid frequency and voltage measurements, response of the system, and communication capability, and so on, are verified on two different type PEV system. Suppression of frequency fluctuation could be confirmed under test conditions close to the real environment.**

Keywords-component; Power System; Electric Vehicle(EV); Vehicle to Grid(V2G); Virtual Power Plant(VPP); Frequency Control; Hardware In the Loop(HIL); Smart Grid

I. INTRODUCTION

Recently, new types of plug-in PEV and PHEV have been announced and released one after another, and which equipped with batteries are widely spreading. Driving distance in normal days is relatively short, so it can be said that V2G is getting real. Various V2G control schemes have been proposed by the simulation study [1], [2], and demonstration projects receiving ancillary service signal from the utility [3], [4]. Last year, the authors conducted an HIL(Hardware In the Loop) using an EV battery test bed and a power conditioner (PCS: Power Conditioning System). The effectiveness of the PEV-FFR(Fast Frequency Response) characterized by high speed response and the PEV-LFC(Load Frequency Control) used mainly for adjusting the thermal power generator was confirmed by test [5].

In this paper, we will introduce the verification test of V2G which is the first case in Japan. We tests V2G control scheme through the HIL(Hardware In the Loop) consisted by a real-time power system simulator assuming massive integration of renewable energy generations and PEVs into the power system, two PEVs with different battery capacities, and two V2G capable power conditioning systems (PCS) with different output, communication and control method.

II. HIL CONFIGURATION AND MODELS

A. Overview of the HIL

Fig. 1 shows the experimental setup in our laboratory, and Fig. 2 shows component of the HIL. The power HIL targeting the EV battery and PCS system [6] is conducted by the frequency fluctuation calculation on the real-time simulator and the power amplifier. Communication HIL is also conducted through the laboratory Ethernet.

Figure 1.   Experimental setup of the HIL.

The frequency value calculated by the power system supply and demand balance calculation model on the real-time simulator (OPAL-RT Technology, OP 5600) is transmitted to the power amplifier (California Instruments, MX 15, rated: 15 [kVA]). The power amplifier reflects the frequency variation value, and outputs the instantaneous voltage value.
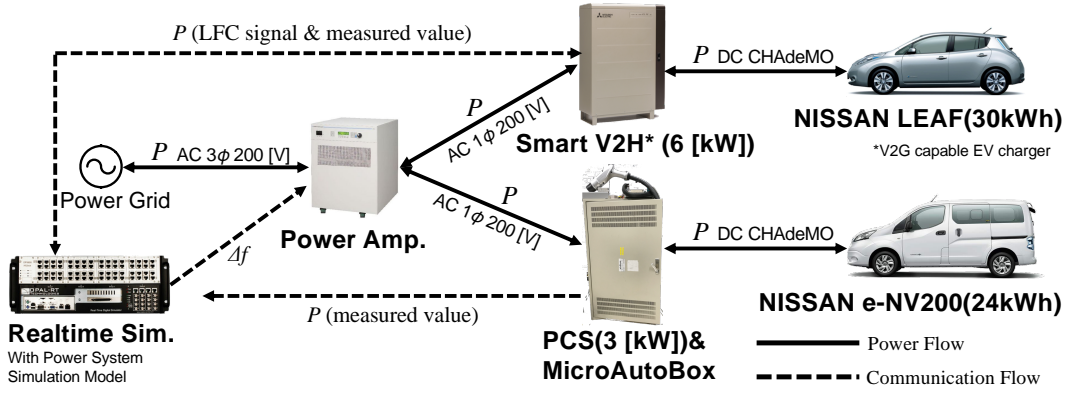
Figure2. Component of the HIL

The control corresponding to FFR is performed by EV controller (dSPACE, Micro Auto Box II) and EV1 (Nissan Motor Co., Ltd., e-NV200 ZAA-ME0, capacity: 24 [kWh]). The EV controller controls and determines V2G power according to its own frequency.

The control corresponding to LFC is performed by "Smart V2H" (Mitsubishi Electric Corporation, EVP-SS60B3-M7-R rated: 6.0 [kW]), which is a household EV charger with built-in PCS equipping V2G function, and EV2 (Nissan Motor Co., Ltd., LEAF ZAA-AZE0 capacity: 30 [kWh]). The Smart V2H receives the LFC command value from the real-time simulator and performs charging and discharging. The communication protocol from the real-time simulator is as shown in Table 1.

In both cases, feeding back measured value of the active power to the real-time simulator, the frequency fluctuation calculation of the next step is performed. This series of operations is repeated in real time.

TABLE I.   COMMUNICATION PROTOCOL OF THE SMART V2H

OSI reference model	Standard
Application layer	ECHONET Lite
Presentation layer	
Session layer	
Transport layer	UDP
Network layer	IP
Data link layer	MAC
Physical layer	Ethernet

B. Simulation and HIL Cases

In order to evaluate each contribution of measurement characteristics, communication delay, and control response, following three cases were assumed.

Case1: HIL test using the EVs and PCS systems.

Case2: Real-time simulation with ideal EV response inside the model.

Case3: Real-time simulation without EV control

Corresponding models and actual hardware are implemented in the real-time simulator at the same time.

C. Power system model

The power system model is assumed to be a prefecture level with a population of about 9 million people. Supply and demand imbalance (ΔP) are calculated by a thermal power generator with EDC (Economic Dispatch Control) and LFC, the PV modeled as natural variation on active power, the aggregated load based on historical measurements, and the EV system, as shown in Fig. 3. The frequency deviation ($\Delta \omega$) is estimated considering the power system inertia constant (M) and the power system damping constant (D). In this paper, system inertia and damping are set as 9 [s], 2 [p.u.], respectively.
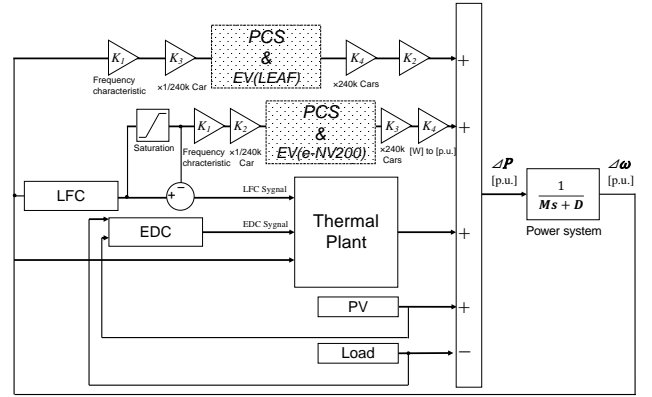
(a) For Case1, 2
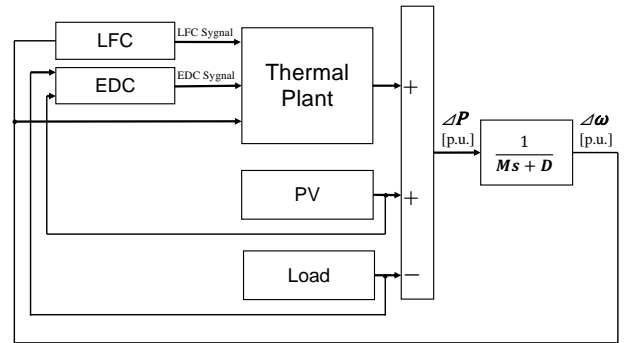
(b) For Case3

Figure 3.   Power system models of each case

Fig. 4. shows the thermal power generator model consists of a turbine and a speed governor, and the parameters are summarized in Table. I [7]. The power output of the thermal power generator is determined based on the EDC, the LFC, and the governor free control. Rate limiter of the LFC and the EDC is 5 [% p.u./min], respectively. The power capacity for the governor-free

control and the LFC is 5 [%] and 1.5 [%] on the system capacity, respectively.
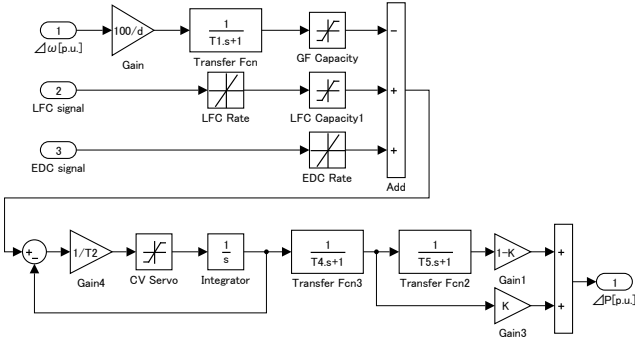
Figure 4.   Thermal power generator model

TABLE II.   PARAMETERS OF THERMAL POWER GENERATOR

d	Permanent Speed Variation [%]	5
T_1	Speed Relay Time Constant [s]	0.2
T_2	CV Servo Time Constant [s]	0.2
T_3	CV Servo Open Time [s]	5
T_4	High Pressure Turbine Time Constant [s]	0.25
T_5	Low Pressure Turbine Time Constant [s]	9.0
T_6	CV Servo Close Time [s]	-0.001
K	High Pressure Output Dispatching Rate [p.u.]	0.3

The EDC signal is simply made from the difference between the demand fluctuation and PV output. Zero-order hold time is 5 [s], and the time constant of the first order lag is set to 30 seconds.

Fig. 5. shows the LFC system model, and the parameter for the LFC is summarized in Table. II. The PI control with anti-windup function is considered to the area requirement estimated by the frequency deviation. In LFC control, the generated LFC signal is preferentially dispatched to the EV, and residual signal is also dispatched to the thermal power generator.
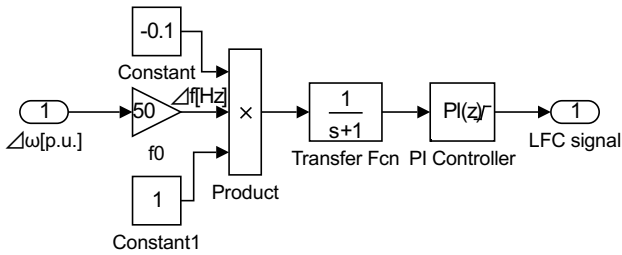
Figure 5.   LFC system model

TABLE III.   PARAMETERS FOR LFC

T_{AR}	Calculation Cycle Time of Area Requirement [s]	1
K_p	PI Controller Proportional Gain [p.u.]	1
T_i	PI Controller Integral Gain [p.u.]	0.1

D. *EV model*

The number of passenger cars owned in the target region is about 3 million. The 2030 target ratio of EV to the total stocks is about 16 %. Therefore, we assumed the number of EVs to be about 480 thousand.

In LFC control, V2G power is determined by the LFC signal. It is assumed that all the EVs receive the same LFC signal. In Case 2, V2G power is determined by the frequency deviation detected at plug-in terminal. Autonomous droop control with 4000 [W/Hz] gain is implemented to the modeled EV and the actual EV(EV1) battery and PCS system.

In this EV test system, 480 thousand cars are equally divided into models with battery capacity of 30 [kWh] and 24 [kWh]. Also, the V2G power is set to 3 [kW] for the FFR control and 6 [kW] for the LFC control according to the PCS rating.

E. *Dataset of PV and Load*

Fig.6 shows dataset of PV power generation and load consumption during a cloudy day. The measurements of actual PV site in every second are used for the HIL. The introduction rate is assumed as 20 % of the system capacity considering Japanese 2030 target. From the viewpoint of protection of experimental equipment, the smoothing effect is simulated by a moving average of 5 seconds. The simulated frequency deviation is higher than that of the current power systems.

The daily trend of the load consumption is generated by using historical dataset published by TEPCO (Tokyo Electric Power Company) [8], [9]. Amount of the load is proportionally divided to a prefecture level. Short cycle load fluctuation is interposed as white noise. Their standard deviation is determined as following well-known relationship.

$$\sigma_D = \gamma\sqrt{P_{demmand}} \qquad (1)$$

Where, γ is set to 0.9 in this paper.
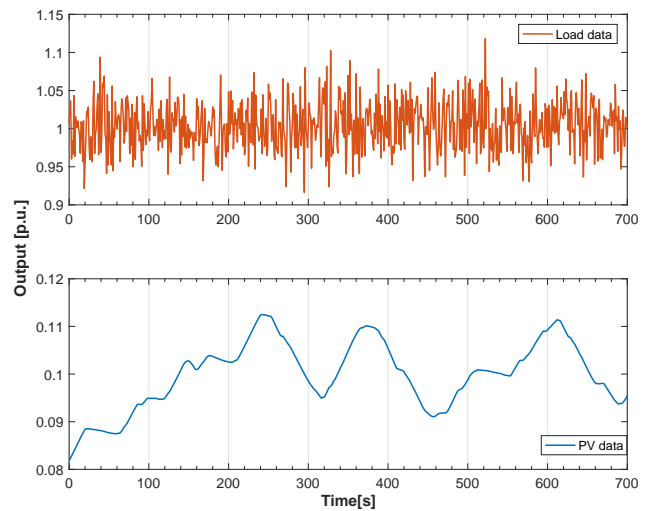
Figure 6.   Dataset of PV and Load

The PV and load dataset of 700 seconds is used for the HIL test because the fluctuation components are significant. Dataset in every second is down sampled and inputted to the 50 [Hz] power system model. Sampling time of the HIL simulation is 0.01 [s], it is enough for considering generator dynamics.

III. RESULTS

The frequency fluctuations of Case 1, Case 2, Case 3 are shown in Fig. 7. There are parts where the frequency fluctuation locally increases and deteriorates. However, due to the control of the EV, the frequency fluctuation can be substantially suppressed.

A comparison on the RMS value basis is shown in Fig. 8. Compared with Case 3 which did not control by EV, the frequency fluctuation can be suppressed by about 31.6 % in Case 2, which is an ideal EV battery simulation, and by about 16.4 % in Case 1 where HIL testing was performed.

The comparison in the histogram is shown in Fig. 9 to Fig. 11. Comparing the frequency around the reference frequency of 50 [Hz] with Case 3 and Case 1, Case 1 in which the HIL test was performed is superior.

Fig. 12 and Fig. 13 show measured values of V2G power obtained by both FFR and LFC control in Case 1. In addition, Fig. 14 shows a comparison between characteristic 30 second frequency and V2G power by both FFR and LFC control. The positive side means charging and the negative side means discharging. From these graphs, the V2G power rise command is issued when the frequency rises, the down command is issued when the frequency is lowered, and the operation is correct. In Fig. 12, the data is interrupted in the vicinity of 200 [s], 400 [s], 460 [s] because the PCS temporarily stops operation.
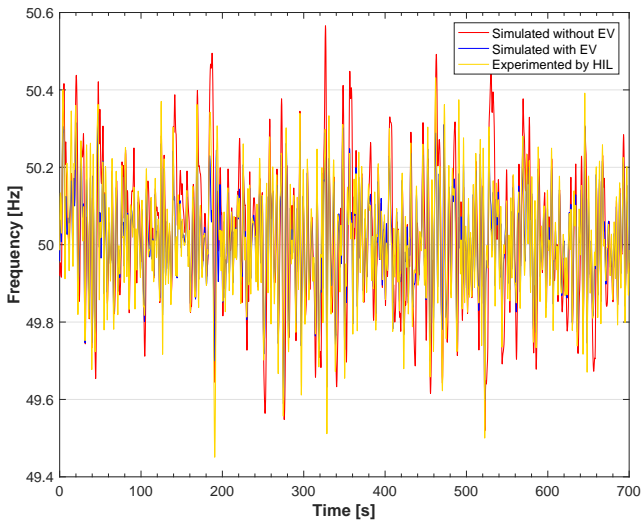
Figure 7.   Frequency fluctuation
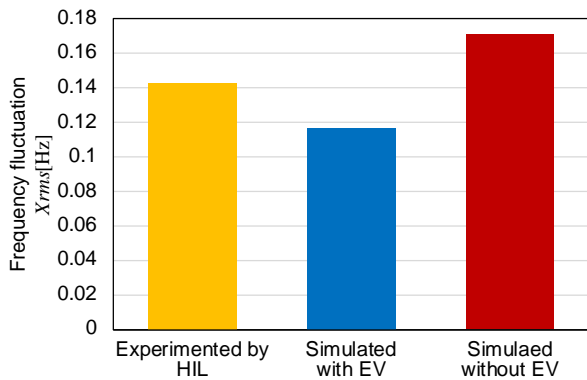
Figure 8.   RMS of frequency fluctuation
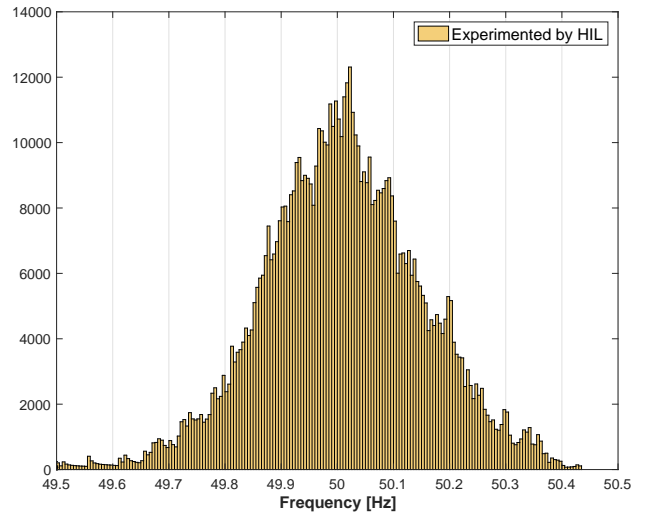
Figure 9.   Histogram of frequency fluctuation (Case1)
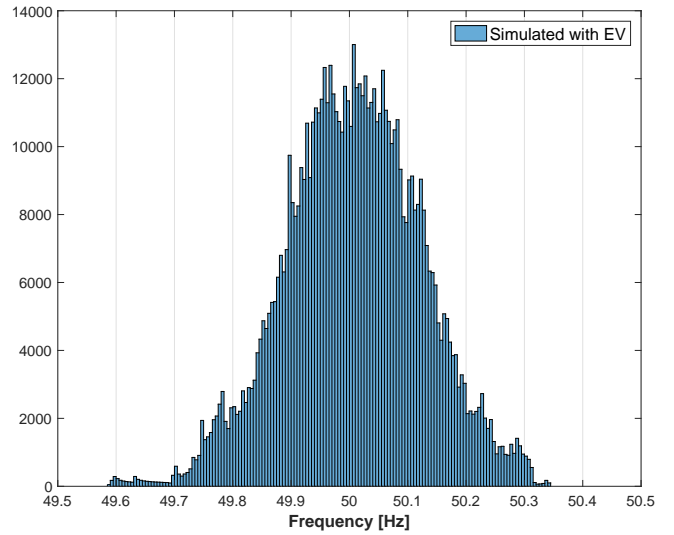
Figure 10. Histogram of Frequency fluctuation (Case2)
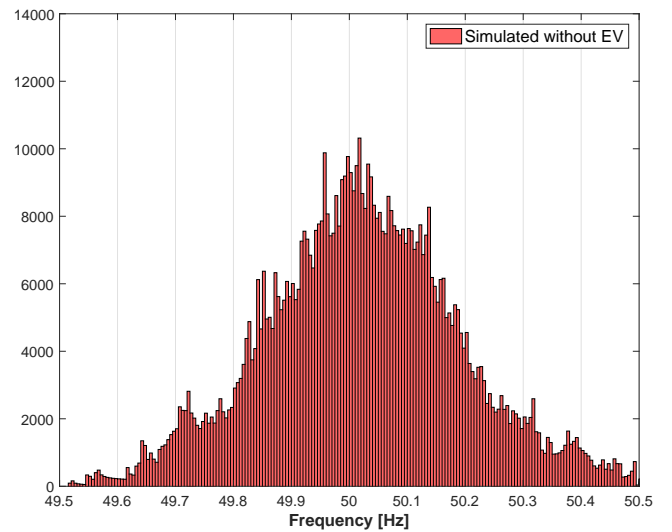
Figure 11. Histogram of frequency fluctuation (Case3)
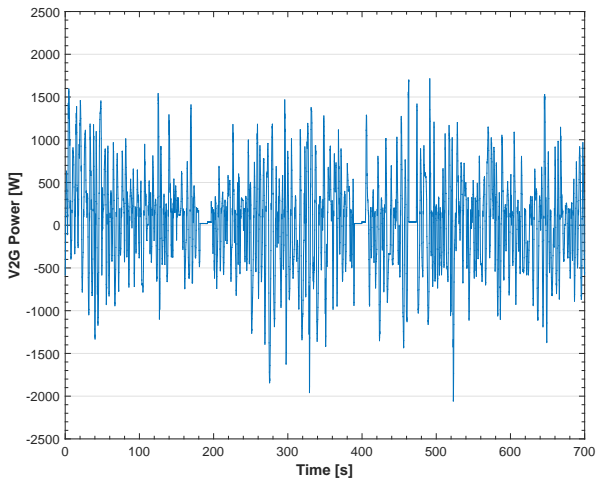
Figure 12. V2G power of FFR control
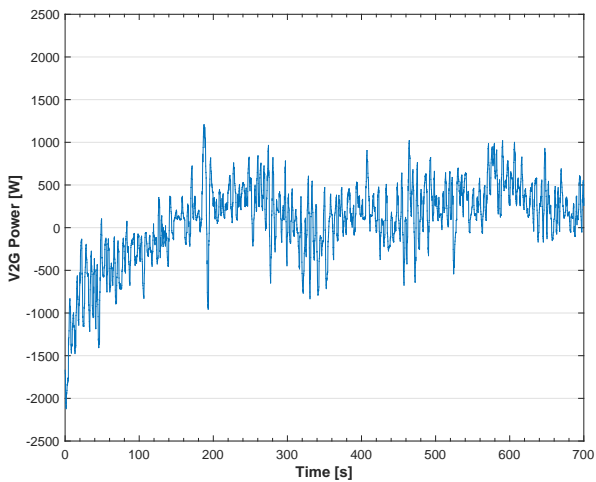
Figure 13. V2G power of LFC control
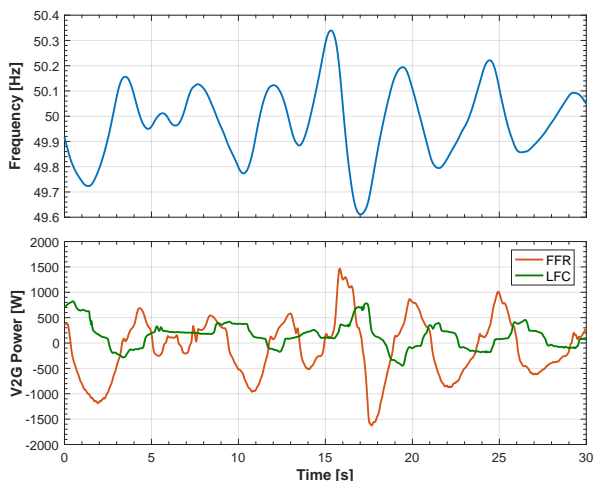
Figure 14. Comparison between frequency fluctuation and V2G power
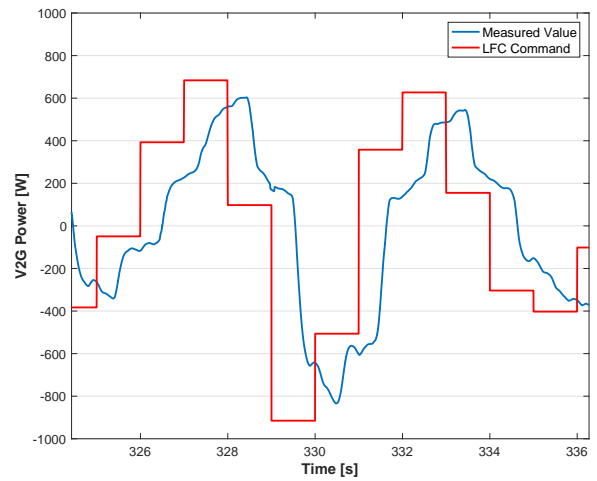
Figure 15. Comparison between LFC command value and measurement value

A comparison between the LFC command value and the measured output value is shown in Fig. 15. The red line is the LFC command value, and the blue line is the measured value. It is conceivable that the command value indicates a stepwise waveform is a problem in terms of communication specification and influences the finish of control. In addition, the delay time between the command value and the measured value was about 0.8 seconds. In the centralized control type LFC, the communication and measurement delay time would be issued, and control performance would be deteriorated depending on the environment.

IV. CONCLUSION

In this paper, we implemented two control methods of centralized control type LFC and autonomous distributed type FFR on different PCS and EVs. Two controls confirmed to be working well from the HILs based on grid integrated supply and demand imbalance calculation with massive renewables and EVs penetration.

We are evaluating control performance of the synthetic inertia response (SIR) based on *df/dt* measurements. Charging and discharging offset control considering differences in SOC (State-of-Charging) is to be designed.

In this time, we tested remote control via the LAN (Local Area Network). It is also conceivable to control the remote PCS via the WAN (Wide Area Network) where the communication delay influences on the control performance.

REFERENCES

[1] M. D. Galus, S. Koch, and G. Andersson, "Provision of Load Frequency Control by PHEVs, Controllable Loads, and a Cogeneration Unit", IEEE Trans. Industrial Electronics, Vol.58, Issue.10, pp.4568-4582 (2011)

[2] E. Sortomme and M. A. El-Sharkawi, "Optimal Combined Bidding of Vehicle-to-Grid Ancillary Services", IEEE Trans. Smart Grid, Vol.3, Issue.1, pp.70-79 (2012)

[3] University of Delaware, "The Grid-Integrated Vehicle with Vehicle to Grid Technology", http://www1.udel.edu/V2G/

[4] The Parker Project, http://parker-project.com

[5] H. Toda, Y. Ota, and T. Nakajima, "HIL Test of Power System Frequency Control by Electric Vehicles", The papers of Technical

Meeting on "Transportation and Electric Railway", IEE Japan, 2017(54-62), pp.37-41 (2017.9.29) (in Japanese)

[6] Y. Ota, H. Taniguchi, J. Baba, and A. Yokoyama, "Implementation of Autonomous Distributed V2G to Electric Vehicle and DC Charging System", Electric Power Systems Research, Vol.120, pp.177–183 (2015)

[7] IEEJ Japanese Power System Models, http://www.iee.jp/pes/?page_id=141

"Load Frequency Control of Power System in Normal and Emergency Case", IEEJ Technical Report, No.869, 2002. (in Japanese)

[8] "Past power usage record data download | Electric weather forecast", TEPCO Power Grid, Incorporated, http://www.tepco.co.jp/forecast/html/download-j.html [January 2017]. (in Japanese)

[9] " Business scale by region | Viewed in a table by TEPCO", Tokyo Electric Power Company Holdings, Incorporated, http://www.tepco.co.jp/corporateinfo/illustrated/business/business-scale-area-j.htm [January 2017]. (in Japanese)